RELIABLE COMPUTATION OF POINTWISE DATA FOR LAMINATED PLATES

P. M. Mohite and C. S. Upadhyay

Department of Aerospace Engineering
Indian Institute of Technology Kanpur, India 208016
mohite@iitk.ac.in, shekhar@iitk.ac.in

1. Introduction

Thin structures made of composite laminates are increasingly used in the manufacture of structural components. The enhanced strength to weight ratios make composites especially attractive for aerospace applications. However, being heterogeneous in nature microscopically, the macroscopic behavior of these structures can be complex. One important aspect of the response of laminated structures that a designer should consider is the onset of failure in a laminated structure. Onset of failure in composite laminated plates requires the local stress state to be known in the structure, particularly near structural details; at interlamina interface and in the individual lamina. Accurate prediction of the local stress state becomes important for a reliable estimate of the failure load, which may be crucial for a safe design of the component.

With an increasing demand to maximize payload carrying capabilities of aerial vehicles, shape and topology optimization of structural components has become an important thrust area. All the optimization problems posed in this context are constrained approximation problem with constraints on failure load, maximum transverse deflection, buckling load, natural frequency, etc. In order to obtain an acceptable optimally designed component, from a computational analysis, it becomes imperative to estimate the constraint quantities accurately, at each step of the optimal design process.

The goal of this study is to determine the quality of the local quantities of interest, obtained using various families of plate models commonly used in engineering practice. The comparisons will be done with respect to the exact three-dimensional elasticity solutions, for both symmetric and anti-symmetric stacking of the laminae. The values of the in-plane stresses obtained directly from the finite element computations will be compared to the elasticity solution. For the transverse stress components, the values obtained from the finite element solution directly, and those obtained using the equilibrium approach of post-processing, will be compared to the exact ones. Further, the study aims at clearly demonstrating the need for proper mesh design in the computation of critical failure loads.

2. Plate Models

Traditionally, for the plate and shell like thin structures, several plate theories have been proposed. These can be broadly classified as:

1. *higher order shear deformable theories (HSDT);*
2. *hierarchic plate theories* and
3. *layerwise theories*

2.1. *Higher Order Shear Deformable Theories (HSDT)*

Here, one such theory due to Reddy[1] is taken as representative theory from this group. It is a third order shear deformable theory with a parabolic distribution of transverse shear strains through thickness of the plate, in order to satisfy the condition of zero transverse shear stress on the top and bottom face of the plate. The HSDT model is denoted by $HDSTp_{xy}$, where p_{xy} denotes the in-plane approximation order.

2.2. *Hierarchic Plate Theories*

In these, the displacement components have a zig-zag or hierarchic representation through the thickness. The hierarchic plate models are a sequence of mathematical models, the exact solutions of which constitute a converging sequence of functions in the norm or norms appropriate for the formulation and objectives of analysis. The construction of hierarchic models for homogeneous isotropic plates and shells was given by Szabó and Sharmann[2] and later for laminated plates by Babuška, Szabó, and Actis[4] and Actis Szabó and Schwab[5]. The solutions of the lower order models are embedded in the highest order model and these models can be adapted according to the requirement.

In these models the displacement field is given as product of functions that depend upon the variables associated with the plate, shell middle surface, and functions of the transverse variable. The transverse functions are derived on the basis of the degree to which the equilibrium equations of three-dimensional elasticity are satisfied. The Fourier transform of the equations of motion is performed which results in two-point boundary value problem for the transverse functions. These are characterized by the geometric parameters and wave vector. These functions are expanded in powers of wave vector around zero. The transverse functions are obtained by solving equations obtained by substituting the expanded functions into the transformed form of equations of motion. The hirrarchic model is denoted by $HRp_{xy}Mm$. Thus HR3M8 denotes hierarchic model with p_{xy}=3 and eight field model.

2.3. *Layerwise Theories*

In these theories, the individual lamina has continuous through thickness representation of displacements. In the present study, the layer-by layer model proposed by Ahmed and Basu[3] is adopted. In this model, all the displacement components are represented as product of in-plane and out-of-plane approximating functions of same order. The hierarchic approximating functions were used. These model are denoted by $LMp_{xy}p_z{}^u p_z{}^v p_z{}^w$. Where, $p_z{}^u = p_z{}^v$ denotes the transverse approximation order for u and v, and $p_z{}^w$ for w. Thus *LM3112* denotes the layerwise model with p_{xy}=3 and $p_z{}^u = p_z{}^v = 1$ and $p_z{}^w$=2.

3. Mathematical Formulation of Plate Models

The generic representation of the displacement field for the plate models is given as:

$$\mathbf{u}(x,y,z) = \begin{Bmatrix} u(x,y,z) \\ v(x,y,z) \\ w(x,y,z) \end{Bmatrix} = [\phi(z)]\mathbf{U}(x,y) \tag{1}$$

where

$$[\phi(z)] = \begin{bmatrix} \phi_1(z) & 0 & \phi_3(z) & 0 & 0 & \phi_6(z) & 0 & 0 & \cdots \\ 0 & \phi_2(z) & 0 & \phi_4(z) & 0 & 0 & \phi_7(z) & 0 & \cdots \\ 0 & 0 & 0 & 0 & \phi_5(z) & 0 & 0 & \phi_8(z) & \cdots \end{bmatrix} \tag{2}$$

and

$$\{U(x,y)\} = \{U_1(x,y)U_2(x,y)U_3(x,y)U_4(x,y)\cdots U_8(x,y)\}^T \tag{3}$$

Note that $U_1(x,y), U_3(x,y), U_6(x,y)\cdots$, ……are the in-plane components of displacement terms $u(x,y,z)$. Similarly, $U_2(x,y), U_4(x,y), U_7(x,y)\cdots$ are the in-plane components of displacement terms $v(x,y,z)$. The in-plane components of transverse displacement $w(x,y,z)$ are given by $U_5(x,y), U_8(x,y)\cdots$. The transverse functions are given in terms of the normalized transverse coordinate $\hat{z} = (2/t)z$ (where t is the thickness of the laminate).

For the higher order shear deformable model the functions $\phi(\hat{z})$ are given as:

$$\phi_1(z) = \phi_2(z) = \phi_5(z) = 1,\ \ \phi_3(z) = \phi_4(z) = z,$$
$$\phi_6(z) = \phi_7(z) = \phi_8(z) = \phi_{11}(z) = 0,\ \ \phi_9(z) = \phi_{10}(z) = z^3$$

Remark: The in-plane displacement components have cubic representation and transverse component is constant in laminate thickness. The quadratic term of in-plane displacement components drop out when the zero shear condition on the top and bottom face of the plate is enforced.

For the hierarchic family of the plate models the transverse functions $\phi(\hat{z})$ are given as

$$\phi_1(\hat{z}) = \phi_2(\hat{z}) = \phi_5(\hat{z}) = 1; \quad \phi_3(\hat{z}) = \phi_4(\hat{z}) = \hat{z}\,\frac{t}{2};$$
$$\phi_6(\hat{z}) = \frac{t}{2}\{\varphi_2(\hat{z}) - \varphi_2(0)\}; \quad \phi_7(\hat{z}) = \frac{t}{2}\{\psi_2(\hat{z}) - \psi_2(0)\}; \quad \phi_8(z) = \frac{t}{2}\{\rho_1(\hat{z}) - \rho_1(0)\};$$
$$\phi_9(\hat{z}) = \frac{t^2}{4}\phi_3(\hat{z}); \qquad \phi_{10}(\hat{z}) = \frac{t^2}{4}\psi_3(\hat{z}); \qquad \phi_{11}(\hat{z}) = \frac{t^2}{4}\rho_2(\hat{z})$$

where

$$\varphi_2(\hat{z}) = \int_{-1}^{\hat{z}} \frac{Q_{44} - Q_{45}}{Q_{44}Q_{55} - Q_{45}^2}\, d\bar{\hat{z}}; \quad \psi_2(\hat{z}) = \int_{-1}^{\hat{z}} \frac{Q_{55} - Q_{45}}{Q_{44}Q_{55} - Q_{45}^2}\, d\bar{\hat{z}};$$
$$\rho_1(\hat{z}) = \int_{-1}^{\hat{z}} \frac{1}{Q_{13}}\, d\bar{\hat{z}}$$

Where Q_{ij} are the coefficients of the global constitutive relation, in the global xyz-coordinate system. For other transverse functions see Ref. 5.

The layerwise model used in this paper is adapted from Ref. 3. The present layerwise plate model is an improvement over the model given in Ref. 3, as the original layerwise model had same order transverse representation for all three displacement components, whereas the present layerwise model can have different approximation in transverse direction for individual displacement components. The different approximation for displacement components is used as suggested by Schwab[6], for a single lamina, to take into account the bending and membrane actions. The displacement component u^l, for an element in the l^{th} layer, is given as

$$u^l(x,y,z) = \sum_{j=1}^{(p_{xy}+1)(p_{xy}+2)} \sum_{k}^{p_z^u+1} u_{jk} N_j^l(x,y) M_k^l(z)$$

where p_{xy} and p_z^u are the in-plane and transverse approximation order (for component u^l) and $N_j(x,y)$ and $\mathrm{M_k(z)}$ are in-plane and transverse approximation functions, respectively. Similarly the other components v^l and w^l can be expressed. The transverse approximation orders for u and v displacement components will be the same, while that for the component w can be different. Hierarchic basis functions will be used for in-plane and transverse representations of the solution components. In this study, $p_{xy} = 2$ or 3 and p_z^u, $p_z^v = 1$, 2, 3 and $p_z^w = 0,$ 1, 2, 3 will be used.

4. Finite Element Formulation

For a given l^{th} lamina, the constitutive relationship in principal material directions is given as:

$$\{\bar{\sigma}_{(l)}\} = [\mathrm{C}_{(l)}]\{\bar{\varepsilon}_{(l)}\} \tag{4}$$

where $\bar{\sigma}_{(l)} = \{\sigma_{11}^{(l)}\ \sigma_{22}^{(l)}\ \sigma_{33}^{(l)}\ \sigma_{23}^{(l)}\ \sigma_{13}^{(l)}\ \sigma_{12}^{(l)}\}^T$ are the stress components for the layer, and $\{\varepsilon_{(l)}\} = \{\varepsilon_{11}^{(l)}\ \ \varepsilon_{22}^{(l)}\ \ \varepsilon_{33}^{(l)}\ \ \gamma_{23}^{(l)}\ \ \gamma_{13}^{(l)}\ \ \gamma_{12}^{(l)}\}^T$ are the components of strain. The subscripts 1, 2 and 3 denote the three principal material directions. The constitutive relationship in global *xyz* coordinates can be obtained by usual transformations.

The potential energy, Π, for the laminate is given by

$$\Pi = \frac{1}{2}\int_V \{\sigma\}\{\varepsilon\}dV \quad -\int_{R^+\cup R^-} q\, w\, ds \tag{5}$$

Where V is the volume enclosed by the plate domain, R^+ and R^- are the top and bottom faces of plate and $q(x,y)$ is the transverse applied load. The solution to this problem $\mathbf{u}_{ex}$ is the minimizer of the potential energy Π. It is obtained by the solution of following weak problem:

Find $\mathbf{u}_{ex} \in H^{\circ}(\mathbf{V})$ such that

$$\mathbf{B}(\mathbf{u}_{ex}, \mathbf{v}) = \mathbf{F}(\mathbf{v}) \quad \forall(\mathbf{v}) \in H^{\circ}(\mathbf{V}) \tag{6}$$

where $H^{\circ}(\mathbf{V}) = \{\mathbf{U} = [\phi]U \mid \mathbf{u}(\mathbf{u}) < \infty \text{ and } \mathbf{MU} = \mathbf{0} \text{ on } \Gamma_D\}$, u is the strain energy with $\mathbf{u} = \frac{1}{2}\mathbf{B}(\mathbf{u},\mathbf{u})$. Here, $\Gamma = \Gamma_N \cup \Gamma_D$ is the lateral boundary of the plate with Dirichlet part Γ_D and Neumann part Γ_N. Note that in this study Dirichlet means the part of lateral boundary where geometric constraints are imposed, while Neumann stands for the stress-free parts of the lateral boundary. Further, **M** depends on the type of Dirichlet conditions on the edge, i.e. soft-simple support; hard simple-support; clamped etc.

Hence, we have

$$\mathbf{B}(\mathbf{u}_{ex}, \mathbf{v}) = \sum_l \mathbf{B}_l(\mathbf{u}_{ex}, \mathbf{v}) = \sum_l \int_{V_l} \{\sigma_{(l)}(\mathbf{u}_{ex})\}^T \{\varepsilon_{(l)}(\mathbf{v})\} dV_l$$

and

$$\mathbf{F}(\mathbf{v}) = \int_{R^+\cup R^-} q v_3 ds \tag{7}$$

where V_l is the volume of the l^{th} lamina in the laminate; v_3 is the transverse component of test function $\boldsymbol{v}$.

5. Error Estimator in the Quantity of Interest

State of stress at a point plays a key role in the first-ply failure analysis of laminates. When the finite element analysis is employed the issue of modeling error (error due to model employed in the analysis of laminate, as compared to three dimensional elasticity) and discretization error becomes important. Adaptive methods for the control of discretization error are available in literature. These are based on the control of energy norm of the error, $\| \mathbf{e} \|_{\Omega} = \sqrt{2\mathsf{u}(\mathbf{e})}$ (where $\mathsf{u}(\mathbf{e})$ is the strain energy of the error). This does not guarantee that the quantity of interest is also accurate. In Ref. 10-Ref. 12 it was shown that the error in the quantity of interest can be given in terms of error in the solution of auxillary problem. Various smoothening based a-posteriori error estimation techniques for laminated composites have been proposed by the authors for the local quantity of interest.[14] Further, estimation and control of the error in the quantity of interest and "one-shot" adaptive approach for the control of discretization error was proposed in Ref. 15 and used for the accurate analysis of first-ply failure loads in Ref. 16. In the present paper the issue of control of modeling error is not addressed. In the following sections the main steps of error estimation for local quantity of interest and one shot adaptivity are given from Ref. 15. Adaptive methods are available in literature for the control of discretization error. The estimation and control of the error in the quantity of interest and "one shot" adaptivity for the control of discretization error was proposed for hierarchic plate models in [1]. Corresponding to the quantity of interest an auxillary problem is solved. Using the estimates for the error in the solution and auxillary problem a-posteriori error estimator for local quantity of interest is defined. Further, for the one shot adaptivity for the quantity of interest the total discretization error is divided into local and pollution error. The desired mesh in local and far field region is obtained to achieve the specified tolerance. The mesh in local region is obtained by repeated refinements till the tolerance is achieved. Thus, the meshes in local and far field region are different.

6. Region-by-region Modeling

6.1 *Imposition of constraints*

In this section the concept of constrained approximation will be discussed. The ideas are generalization of the concept introduced in [7]. In order to fix ideas let us consider a one-dimensional example. Let us take on interval (0, L) with one element, as shown in Fig.7 (a). Let us also assume that piecewise linear basis functions (i.e. p = 1) are defined over this mesh.
Let

$$v(z) = \sum_{i=1}^{p+1} a_i M_i(z)$$

Be the representation of a function over this domain. Here, M_1 (z) are the linear basis functions defined as shown in Fig. 7(a). Let us now subdivide this element into two equal sub-elements, let the function v (z), given above, be represented in terms of the piecewise linear basis functions (as shown in Fig. 7(b)). As

$$v(z) = \sum_{i=1}^{2p+1} a_i M_i(z)$$

Where, $\overline{M}_1\ (z)$ are the piecewise linear basis functions defined over the new mesh. Since both equations 5 and 6 represent the same function, the coefficients $\overline{a}_1$ can be expressed in terms of the coefficients a_j. It is obvious that

$$\overline{a}_1 = a_1; \quad \overline{a}_2 = \frac{a_1 + a_2}{2}; \quad \overline{a}_3 = a_2$$

Similarly, the representation of v (z) over any finer mesh can be obtained in terms of the representation over the coarser mesh, with the new fine mesh coefficients $\overline{a}_j$ constrained by the values of the coefficients a_i for the coarser mesh. This can be easily extended to any p-order approximation defined over the coarser and fine meshes. As shown below, the transverse representation of the finite element solution is defined over a group. However, the basic building block in the analysis is the individual three-dimensional element τ_{3D}. Hence, the approach given above will be employed to represent the element degrees of freedom in terms of the group degrees of freedom.
The region-by-region model is denoted by $RRMp_{xy}p_z{}^u p_z{}^v p_z{}^w$.

6.2 *Implementation for Region-by-region Model*

The eq. (4) can be rewritten as

$$\Pi = \sum_{\tau} \frac{1}{2} \{u^\tau\}^T [K^\tau] \{u^\tau\} - \{u^\tau\}^T \{F^\tau\}$$

Where, $\{u^\tau\}$ denotes the displacement vector, $[K_\tau]$ denotes the stiffness matrix and $\{F^\tau\}$ denotes the load vector corresponding to element $\tau_{3D}\,(or\ \tau)$. Using eq. 15, to represent $\{u^\tau\}$, eq. (22) reduces to

$$\Pi = \sum_{\tau} \frac{1}{2} \{u^G\}^T [A^\tau]^T [K^\tau] [A^\tau] \{u^G\} - \{u^G\}^T [A^\tau]^T \{F^\tau\}$$

Minimization of Π gives the solution for $\{u^G\}$. Note that this gives the element stiffness matrix $[\overline{K}^\tau]$ and load vector $\{\overline{F}^\tau\}$ in terms of the constraint matrix, as

$$[\overline{K}_\tau] = [A^\tau]^T [K^\tau][A^\tau]; \quad \{\overline{F}^\tau\} = [A^\tau]^T \{F^\tau\}$$

7. Effect of Models on Accuracy of Pointwise Data

7.1 *Comparison of Transverse Deflection*

In this section the transverse deflection component obtained using different plate models and in-plane discretization is compared with the exact three-dimensional elasticity results reported in Ref. 19, for cross-ply laminate sequence with material properties given in Table 1. The plate has dimension a along x-axis and b along y-axis, and is subjected to sinusoidal loading of the form

$$q(x,y) = q_0(x,y)\sin\left(\frac{\pi x}{a}\right)\sin\left(\frac{\pi y}{b}\right) \quad (29)$$

All edges of the plate are hard simply supported. The transverse deflection at $\left(\frac{a}{2},\frac{b}{2},0\right)$ is reported in Tables 3 and 4. The models used are *HSDT3*, *HR3M11* and *LM3332*. Square plate with cross ply laminae, such that outer laminae have orientation 0°, and total thickness of 0° laminae is equal to total thickness of 90° laminae. Also laminae with same orientation have equal thickness. In this study, 7 and 9-layered laminate is studied. The transverse deflection is normalized as $w^* = \frac{\pi^4 Q w}{12 q_0 S^4 t}$, where $Q = 4G_{12} + \left[E_{11} + E_{22}\left(1 + 2\nu_{23}\right)\right]/\left(1 - \nu_{12}\nu_{21}\right)$. Numbers in parenthesis show the % error with respect to exact solution.

From tables 3 and 4 we observe that:

1. The *LM3332* model predicts the transverse deflection accurately for all the aspect ratios. The error in the values ranges from 0-0.15 %.
2. The *HSDT3* and *HR3M11* model are far from the exact one for the aspect ratios upto $S = 10$. The error for this aspect ratios ranges from 5-16 %.
3. For the *HSDT3* and *HR3M11* model with aspect ratios $S > 10$ the displacement is close to exact. The error is 0.1-3 %.
4. The *HR3M11* model is closer to the exact one; as compared to the *HSDT3* model.

Table 3:Non-dimensional transverse deflection $\left(w^*\right)$ for 7 layered cross-ply laminate.

S	Pagano[19]	Layer-wise	HSDT	Hierarchic
2	12.342	12.341 (0.00)	10.918 (11.54)	10.358 (16.07)
4	4.153	4.153 (0.00)	3.594 (13.46)	3.575 (13.92)
10	1.529	1.529 (0.00)	1.417 (7.33)	1.444 (5.56)
20	1.133	1.133 (0.00)	1.096 (3.26)	1.113 (1.76)
50	1.021	1.021 (0.00)	1.005 (1.56)	1.017 (0.39)
100	1.005	1.005 (0.00)	0.993 (1.19)	1.004 (0.09)

Table 4:Non-dimensional transverse deflection $\left(w^*\right)$ for 9 layered cross-ply laminate.

S	Pagano[19]	Layer-wise	HSDT	Hierarchic
2	12.288	12.306 (-0.15)	10.703 (12.89)	11.632 (5.34)
4	4.079	4.079 (0.00)	3.530 (13.46)	3.664 (10.17)
10	1.512	1.512 (0.00)	1.406 (7.01)	1.438 (4.89)
20	1.129	1.129 (0.00)	1.093 (3.18)	1.110 (1.68)
50	1.021	1.020 (0.09)	1.001 (1.96)	1.017 (0.39)
100	1.005	1.005 (0.00)	1.004 (0.09)	0.993 (1.19)

7.2 *Comparison of Stresses*

Case 1: In this case [0/90/0], square laminate with all edges simple supported is considered. All the laminae are of equal thickness. The sinusoidal loading is of the same form as above. The in-plane stresses given in [] are normalised as $\left(\bar{\sigma}_{xx},\bar{\sigma}_{yy},\bar{\tau}_{xy}\right)=\frac{1}{q_0 S^2}\left(\sigma_{xx}\left(\frac{a}{2},\frac{b}{2},\bar{z}\right),\sigma_{yy}\left(\frac{a}{2},\frac{b}{2},\bar{z}\right),\tau_{xy}\left(0,0,\bar{z}\right)\right)$ and the transverse stresses as $\left(\bar{\tau}_{xz},\bar{\tau}_{yz}\right)=\frac{1}{q_0 S}\left(\tau_{xz}\left(0,\frac{b}{2},\bar{z}\right),\tau_{yz}\left(\frac{a}{2},0,\bar{z}\right)\right)$. The in-plane stress components are shown in Fig. 3 and transverse stress component is shown in Fig. 4. The models used are *HSDT3*, *HR3M11* and *LM3332*.

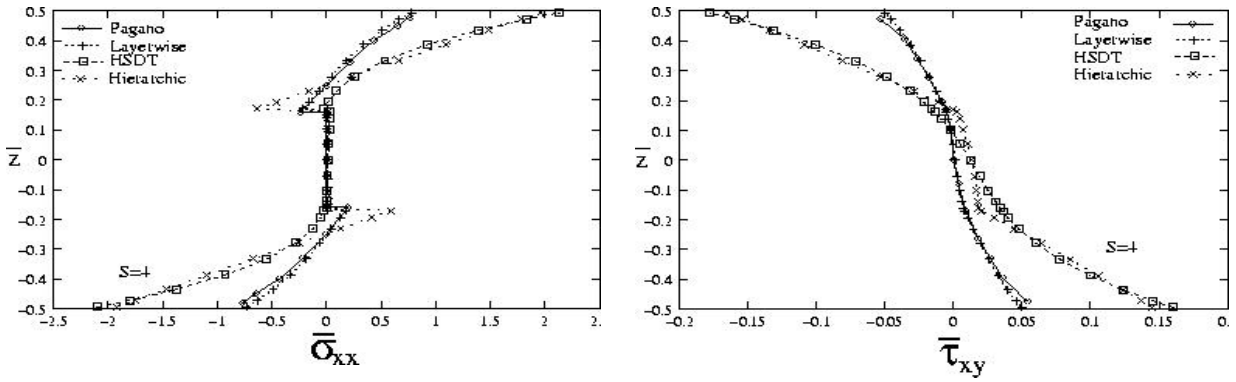

Fig. 3 [0/90/0] laminate; all edges simply supported, in-plane stresses.

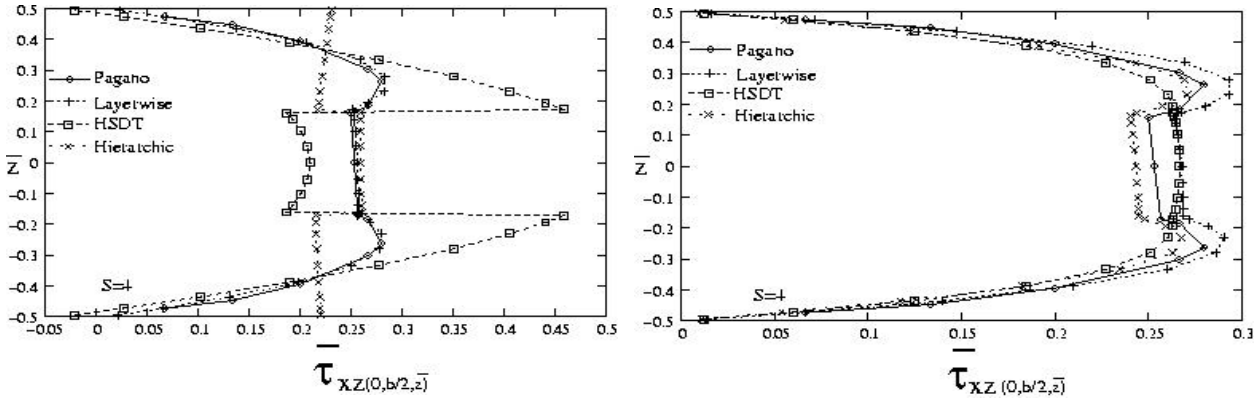

Direct stresses Equilibrium stresses

Fig. 4 [0/90/0] laminate; all edges simply supported, transverse stresses.

Case 2: In this case the [165/-165] laminate under cylindrical bending is considered. The transverse load applied is of the form $q(x,y)=q_0(x)\sin\left(\frac{\pi x}{a}\right)$. The laminate with *S=4* with the edges *x=0, a/2* are simple supported and infinite along *y*-direction. The transverse stress $\bar{\tau}_{xz}\left(0,\bar{z}\right)$ is shown is fig. *. In the region-by-region model used here, one layer of elements at (0,b/2) (where the stress is plotted) uses the *LM3332* and remaining domain of the laminate uses *EQ3112*. The other models used are *HSDT3*, *HR3M11* and *LM3332*.

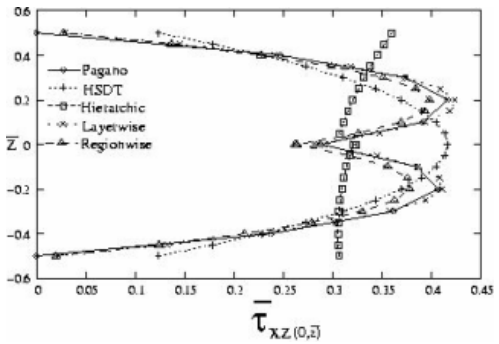

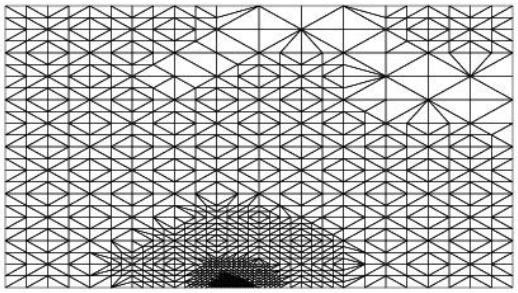

Effect of Models on Accuracy of Predicted Failure Load

The laminates considered are $[0/90]_S$ and [-45/45/-45/45]. The plate is either clamped on all edges or simple supported. The top face of the plate is subjected to uniform transverse load $q(x,y)=q_0$. The plate dimensions are $a=228.9\ mm\ (9\,in)$ and $b=127\ mm\ (5\,in)$. The material properties are given in Table 7. The first-ply failure load is nondimensionalised as $FLD=\frac{q_0}{E_{22}}S^4$. The results obtained from the present analysis are compared with those reported in Ref. 22.

Table 11: First-ply failure loads; all edges clamped, [-45/45/-45/45] laminate under uniform transverse loading, (equilibrium stresses) $p_{xy}=2$.

Model	FLD	Xco	Yco	Layer	Location	FI_{TW}	Max. σ
Reddy[22]	39354.8	≈115.0	≈125.0	1	bottom	-	
HSDT[a]	31463.7	107.51	0.56	4	top	1.00	σ_{22}
HSDT[b]	31463.7	112.71	0.14	4	top	1.82	
HSDT[c]	23377.6	112.71	0.14	4	top	1.00	
5-field[a]	31486.1	107.51	0.56	4	top	1.00	σ_{22}
5-field[b]	31486.1	112.71	0.14	4	top	1.82	
5-field[c]	23383.7	112.71	0.14	4	top	1.00	
8-field[a]	31403.1	107.51	0.56	4	top	1.00	σ_{22}
8-field[b]	31403.1	112.71	0.14	4	top	1.82	
8-field[c]	23350.7	112.71	0.14	4	top	1.00	
11-field[a]	31672.2	121.38	126.43	4	top	1.00	σ_{22}
11-filed[b]	31672.2	116.18	126.85	4	top	1.75	
11-field[c]	23955.1	116.18	126.85	4	top	1.00	
Layer	32549.2	107.51	0.56	1	bottom	1.00	σ_{22}

Table 15: First-ply failure loads; all edges simple supported, [-45/45/-45/45] laminate under uniform transverse loading, (equilibrium stresses) $p_{xy}=2$.

Model	FLD	Xco	Yco	Layer	Location	FI_{TW}	Max. σ
Reddy[22]	32513.5	≈115.0	≈65.0	4	top	-	

HSDT[a]	25802.4	138.28	66.13	4	top	1.00	σ_{22}
HSDT[b]	25802.4	136.99	73.26	4	top	1.08	
HSDT[c]	24729.1	136.99	73.26	4	top	1.00	
5-field[a]	25807.7	90.62	60.86	4	top	1.00	σ_{22}
5-field[b]	25807.7	91.91	53.73	4	top	1.09	
5-field[c]	24729.5	91.91	53.73	4	top	1.00	
8-field[a]	25687.1	90.62	60.86	4	top	1.00	σ_{22}
8-field[b]	25687.1	91.91	53.73	4	top	1.08	
8-field[c]	24727.7	91.91	53.73	4	top	1.00	
11-field[a]	30791.5	31.22	0.56	4	bottom	1.00	σ_{22}
11-filed[b]	30791.5	0.25	0.96	4	top	1.39	
11-field[c]	26173.7	0.25	0.96	4	top	1.00	
Layer	31078.2	1.20	107.16	4	top	1.00	σ_{22}

With equilibrium stresses we observe that:

1. For the initial mesh, the failure loads predicted by all the models are lower than those obtained in Ref. 22 (shown with superscript a) and those obtained by using direct stresses.
2. The locations predicted by all the models are either close to one obtained in Ref. 22 or are corresponding symmetric points.
3. Failure loads predicted by the HSDT and hierarchic models are close while those predicted by layerwise are slightly higher than these.
4. When the discretization error control is used the failure index, for the failure load obtained using adapted mesh, increases upto 85%. This is due to the increased flexibility of the numerical solution for the adapted mesh.
5. With the adapted mesh the error in the failure load computations can be close to 25%.
6. The failure locations for the HSDT and hierarchic models are in the same region before and after the use of discretization error control.

Thin laminated structures are widely used in aerospace component designs. Reliable computation of pointwise data plays an important role in design, optimization and certification phase. Many plate models are available in literature but not much can be said about the accuracy of pointwise data like stress state and displacements which may the quantity of interest for an optimal design.

The above concept is used in the prediction of first-ply failure load for laminates, which is common engineering design practice. Here, the quantity of interest is the stress component, which contributes maximum towards the first-ply failure index (see [2], [3]). It is seen that the first-ply failure load goes down by 40% when discretization error control using focussed adaptivity is used.

A layerwise model is developed for the analysis of laminates. Further, a regionwise model is developed which combines the advantage of accurate computation of layerwise model in the region of interest and economy of computations of equivalent single layer models in the far region, yet maintaining the accuracy.

Figure 1. (a) Adapted mesh (b) Transverse shear stress

Reference

[1] Ahmed, N. U., and Basu, P. K., "Higher-order finite element modeling of laminated composite plates," International Journal of Numerical Methods in Engineering, Vol. 37, 1994, pp 123, 129.

[2] Actis R. L., Szabó, B. A., and Schwab C., "Hierarchic models for laminated plates and Shells," Computer Methods in Applied Mechanics and Engineering, Vol. 172, 1999, pp. 79, 107.

[3] Schwab, C., "A-Posteriori Modeling Error Estimation for Hierarchic Plate Model," Numerische Mathematik, Vol. 74, 1996, pp. 221. 259.

[4] PM. Mohite, and CS. Upadhyay, "Focussed adaptivity for laminated plates," *Computers and Structures,* v. 81, p. 287-293, 2003.

[2] PM Mohite and CS. Upadhyay, "Reliable computation of local quantities of interest in composite laminated plates," *46th AIAA/ASME/ASCE/AHS/ASC Structures, Structural Dynamics & Materials Conference*. Austin, Texas, 18-21st April, 2005.

[3] PM. Mohite and CS. Upadhyay, "Accurate computation of critical local quantities in composite laminated plates under transverse loading," Communicated to *Computers and Structures*.